A Finite Volume Procedure for Thermo-Fluid System Analysis in a Flow Network

Alok Majumdar
NASA/Marshall Space Flight Center
Huntsville, Alabama

Abstract

This paper describes a finite volume procedure for network flow analysis in a thermo-fluid system. A flow network is defined as a group of inter-connected control volumes called "nodes" that are connected by "branches". The mass and energy conservation equations are solved at the nodes and momentum conservation equations are solved at the branches. The flow network also includes solid nodes to account for fluid to solid heat transfer. The heat conduction equation is solved at the solid nodes in conjunction with the flow equations. The properties of a real fluid are calculated using a thermodynamic property program and used in the conservation equations. The system of equations describing the fluid-solid network is solved by a hybrid numerical method that is a combination of the Newton-Raphson and successive substitution method. This procedure has been incorporated into a general-purpose computer program, the Generalized Fluid System Simulation Program, GFSSP. This paper also presents the application and verification of the method by comparison with test data for several applications that include (a) internal flow in a rocket engine turbo-pump, (b) pressurization and loading of a cryogenic propellant tank, (c) fluid transient during sudden opening of valve for priming of an evacuated feed line, and (d) chilldown of a cryogenic transfer line with phase change and two phase flows.

1. Introduction

The need for a generalized numerical method for thermo-fluid analysis in a flow network has been felt for a long time in the aerospace industry. Designers of thermo-fluid systems often need to know pressures, temperatures, flowrates, concentrations, and heat transfer rates at different parts of a flow circuit for steady state or transient conditions. Such applications occur in propulsion systems for tank pressurization, internal flow analysis of rocket engine turbo-pumps, chilldown of cryogenic tanks and transfer lines and many other applications of gas-liquid systems involving fluid transients and conjugate heat and mass transfer. Computer resource requirements to perform time-dependent three-dimensional Navier-Stokes Computational Fluid Dynamic (CFD) analysis of such systems are prohibitive and therefore are not practical. A possible recourse is to construct a fluid network consisting of a group of flow branches such as pipes and ducts that are joined together at a number of nodes. They can range from simple systems consisting of a few nodes and branches to very complex networks containing many flow branches simulating valves, orifices, bends, pumps and turbines. In the analysis of existing or proposed networks, node pressures, temperatures and concentrations at the system boundaries are usually known. The problem is to determine all internal nodal pressures, temperatures, and

concentrations, as well as branch flow rates. Such schemes are known as Network Flow Analysis methods, and they use largely empirical information to model fluid friction and heat transfer. The oldest method for systematically solving a problem consisting of steady flow in a pipe network is the Hardy Cross method [1]. The original method was developed for hand calculations, but it has also been widely employed for use in computer-generated solutions. But as computers allowed much larger networks to be analyzed, it became apparent that the convergence of the Hardy Cross method was very slow or even failed to provide a solution in some cases. The other limitation of this method is its inability to extend to unsteady, compressible flow and heat transfer.

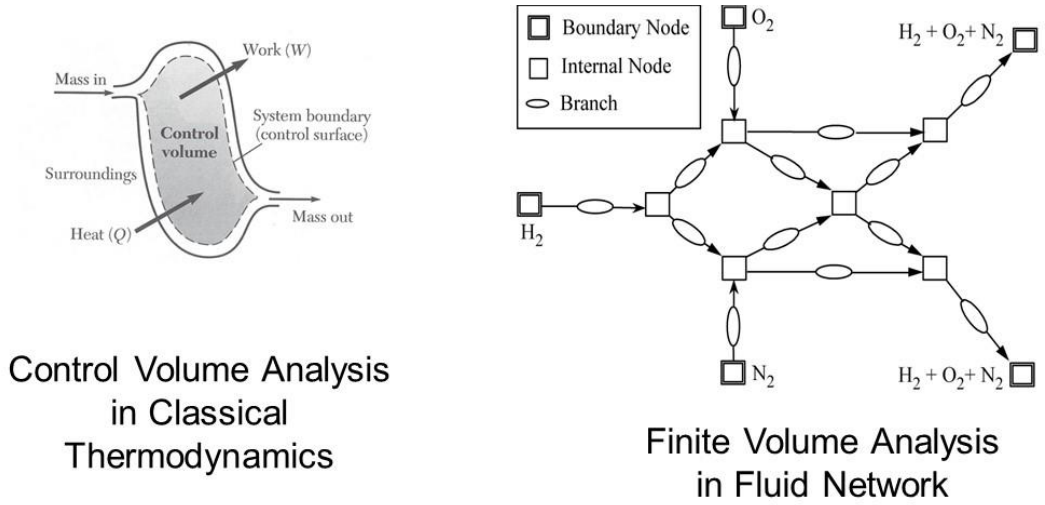

Figure 1. Extension of Control Volume Analysis to Finite Volume Analysis in Fluid Network

Finite volume procedures are an extension of the control volume analysis performed in classical thermodynamics for mass and energy conservation (Figure 1). Therefore, a finite volume procedure is a logical choice for solving network flow which is a collection of inter-connected control volumes. Finite volume procedure was first developed by Professor Spalding and his students at Imperial College [2] to solve the Navier-Stokes equations in two dimensions. The Navier-Stokes equations were expressed in terms of stream function and vorticity using an upwind scheme [3] to ensure numerical stability for high Reynolds number flows. The governing equations are derived using the principle of conservation of variables. The system of equations was solved by a successive substitution method. This method was successfully applied to solve many recirculating flows which were never solved before. The Navier-Stokes equation in three dimensions was solved in its primitive form by Patankar and Spalding [4]. They used a staggered grid where pressures were located at the center of the control volume whereas velocities were located at the boundaries of the control volume. This finite volume procedure was known as the SIMPLE (Semi-Implicit Pressure Linked Equation) algorithm. It uses the mass conservation equation to develop pressure corrections using a simplified momentum equation. The pressures and velocities are corrected iteratively until the solution is converged. Turbulence was modeled by defining an effective viscosity which is a function of turbulence properties such as turbulence energy and its dissipation rate and known as

Launder and Spalding's [5] k-ε model of turbulence. The turbulence model equations are solved in conjunction with the mass and momentum conservation equations. The SIMPLE algorithm and two-equation model of turbulence have been implemented in many Computational Fluid Dynamics (CFD) codes in later years.

Navier-Stokes based CFD codes, however, are not suitable for thermo-fluid system analysis. It is not practical to solve for three dimensional Navier-Stokes equations in conjunction with turbulence model equations to model a thermo-fluid system consisting of many fluid components such as pumps, pipes, valves, orifices and bends. On the other hand, it is possible to solve a one-dimensional momentum equation with empirical correlations to model frictional effect to determine flow and pressure distribution in a flow network consisting of many such fluid components within reasonable computer time. A modified form of the SIMPLE algorithm was used to compute flow distribution in manifolds [6,7], where one-dimensional mass and momentum equations were solved using the Colebrook equation [8] for friction factor to account for viscous effect. Numerical predictions compared well with experimental data. However, this approach cannot be extended for any given flow network. A generalized flow network cannot be constructed using a structured co-ordinate system. In order to develop a numerical method to analyze any given flow network, the conservation equations for mass, momentum and energy must be written using an unstructured co-ordinate system. This paper presents a finite volume procedure for calculating flow, pressure and temperature distribution in a generalized fluid network for steady-state, transient, compressible, two-phase and with or without heat transfer. The thermo-fluid system network is discretized into fluid nodes and branches, solid nodes and conductors. The fluid nodes are connected with branches, and scalar properties such as pressure, enthalpy and concentrations are stored in the fluid nodes, and vector properties such as flowrates and velocities are stored in the branches. Solid nodes and fluid nodes are connected by solid to fluid conductors. The conservation equations for mass and energy are solved at fluid nodes and momentum conservation equations are solved at fluid branches in conjunction with the thermodynamic equation of state for real fluids. The energy conservation equation for a solid is solved at the solid nodes. The system of equations is solved by a hybrid numerical method which consists of both the Newton-Raphson and Successive Substitution methods. This procedure has been incorporated into a general purpose computer program, GFSSP (Generalized Fluid System Simulation Program) [9-11]. This paper describes several applications of GFSSP that include (a) internal flow in a rocket engine turbo-pump, (b) compressible flows in ducts and nozzles, (c) pressurization and loading of a cryogenic propellant tank, (d) fluid transient during sudden opening of a valve for priming of a partially evacuated propellant feed line, and (e) chilldown of cryogenic transfer line with phase change and two phase flows.

2. Mathematical Formulation

The mathematical formulation to solve numerically the flow in a network offers a different kind of challenge than solving the Navier-Stokes equations in three dimensions. The Navier-Stokes equations are usually written for the co-ordinate systems which are topologically Cartesian. In a topologically Cartesian system of co-ordinates, a control

volume can have a maximum of six neighboring control volumes: east, west, north, south, high and low. The data structure for a three dimensional co-ordinate system can be adapted for deriving the conservation equations for mass, momentum and energy. On the other hand, a fluid network cannot be fully represented in a three dimensional Cartesian co-ordinate system which has a limitation on the maximum number of neighbors. A fluid network is n-dimensional where n can assume any number. Therefore, its data structure is unique. In the following section the network definition and data structure of a flow network will be described. This will be followed by the description of governing equations which will include the conservation equations of mass, momentum, energy, and mixture species, as well as auxiliary equations such as the thermodynamic equation of state and empirical equations for friction and heat transfer.

2.1 Network Definitions

A flow network is first discretized into nodes and branches prior to the development of the governing equations. The defining parameters of a network are explained with the help of the example of a counter-flow heat exchanger shown in Figure 2. In this example hot fluid in the central tube is cooled by cold fluid in the annulus. The two fluid streams are exchanging energy by heat conduction and convection. This physical system is represented by a network of fluid and solid nodes. The fluid paths in the central tube and annulus are represented by a set of internal and boundary fluid nodes connected by fluid branches. The branch represents a fluid component such as a pipe, orifice, valve or pump. In this particular case the pipe and annulus are chosen as branch options. The mass and energy conservation equations are solved at the internal fluid nodes and the momentum equations are solved at the branches. It may be noted that this concept is similar to the staggered grid concept of the SIMPLE algorithm [4]. The walls, through which heat is transferred from hot fluid to cold fluid, are discretized both axially and radially. Solid to fluid conductors connect solid and fluid nodes and calculate the convective heat transfer rate, and solid to solid conductors connect solid nodes and calculate conduction heat transfer. The energy conservation of a solid is solved at the solid nodes accounting for heat transfer with neighboring solid and fluid nodes.

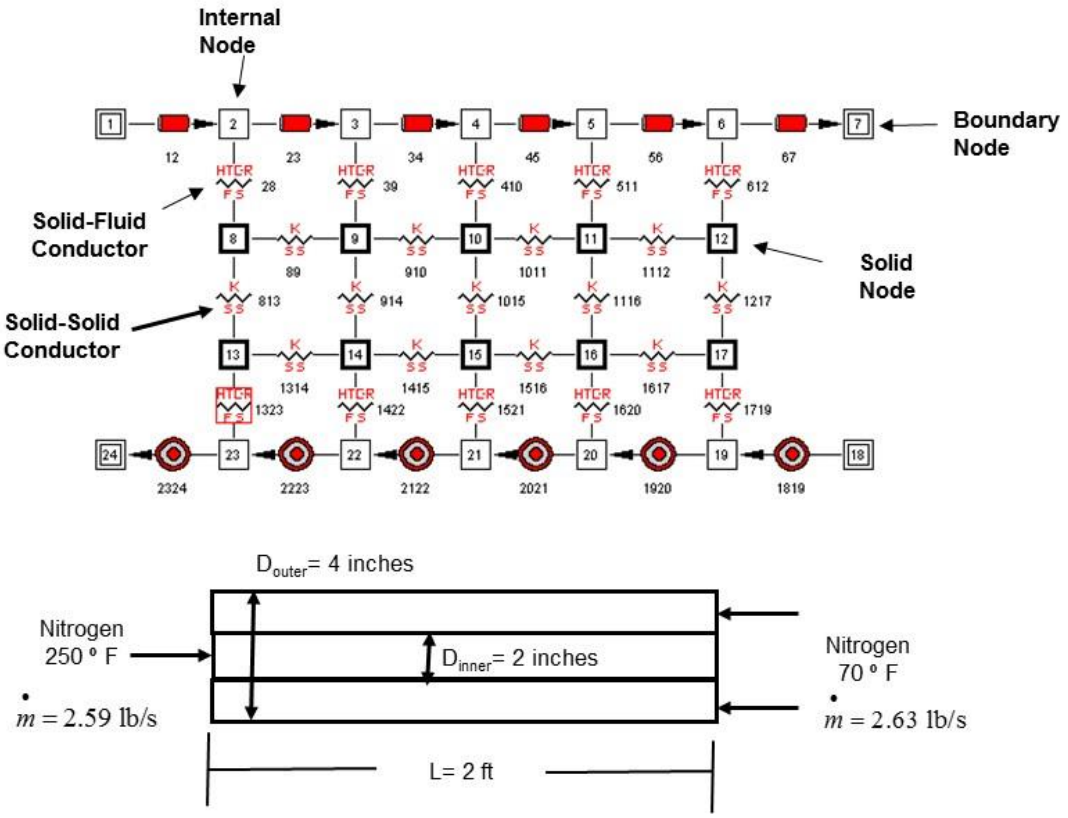

Figure 2. Flow network representing a counter-flow heat exchanger

2.2 Data Structure

In a flow network, the layout of the nodes cannot be represented by a structured co-ordinate system (Figure 1). There is no origin and no preferred co-ordinate direction to build the network of nodes and branches. In a structured co-ordinate system, the array of nodes can be constructed in the pre-specified co-ordinate direction. In 1-D flow network, each node has two neighbors; in 2-D flow network, each node has four neighbors and in 3-D flow network, each node has six neighbors. In a typical flow network, a node can have "n" number of neighbors. Therefore, a unique data structure needs to be developed to define an unstructured flow network.

Any flow network can be constructed with three elements: 1) Boundary Node, 2) Internal Node and 3) Branch. Each element has properties. Internal nodes and branches, where the conservation equations are solved, have two kinds of properties: Geometric and Thermo-fluid. There are two types of geometric properties: relational and quantitative. The data structure of the flow network is shown in Figure 3. The relational geometric property allows nodes and branches to know their neighbors. Thermo-fluid properties include pressure, temperature, enthalpy, density, viscosity, etc.

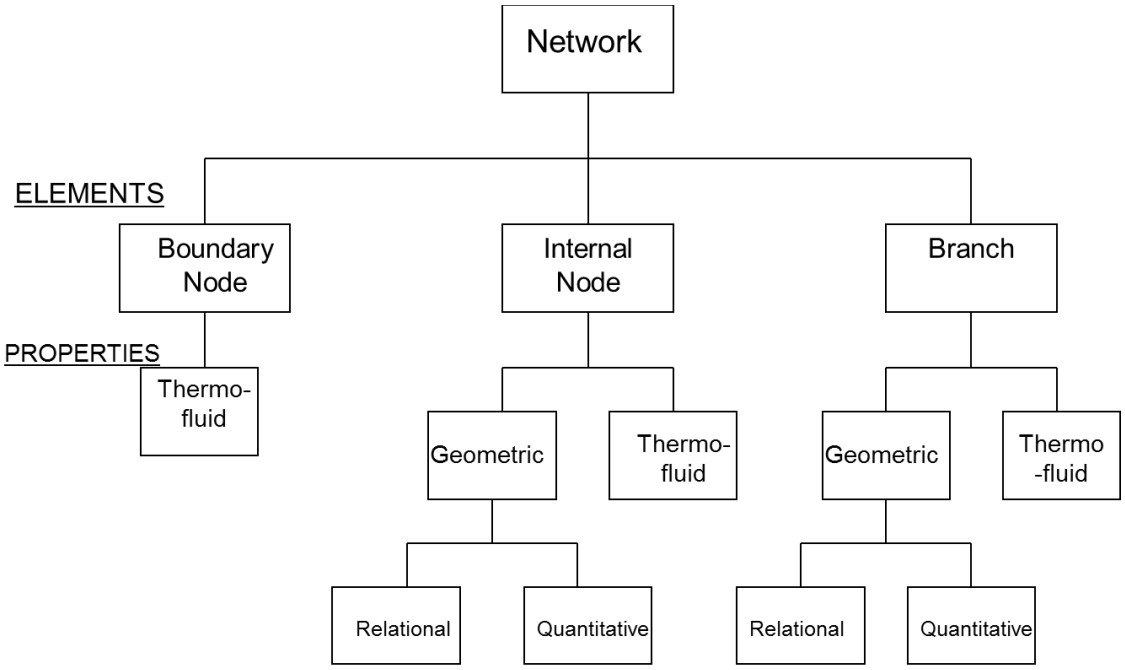

Figure 3. Data Structure for Network Flow Analysis

Each node is designated by an arbitrary number and assigned a pointer to the array where node numbers are stored. The pointers are necessary to access the thermodynamic and thermo-physical properties of the node. The relational properties of the node include the number of branches connected to it and the names of those branches. Figure 4 shows an example of these two relational properties of a node in a given network.

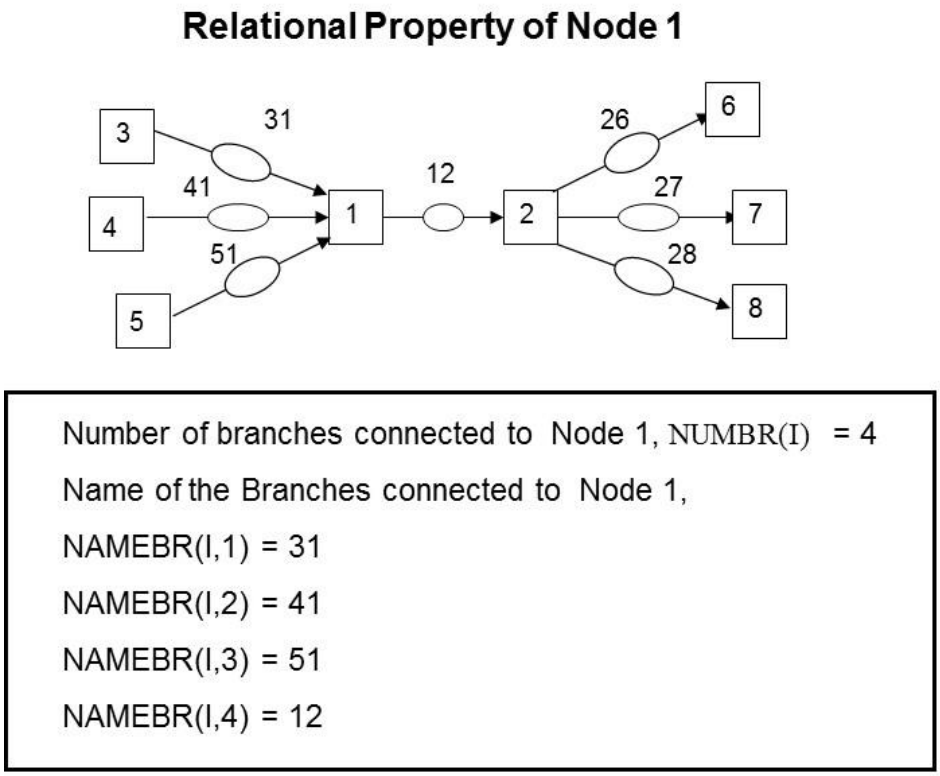

Figure 4. Example of Relational Property of a Node

Like the nodes, each branch is also designated by an arbitrary number and assigned a pointer to the array where branch numbers are stored. The relational properties of the branch include a) the names of the upstream and downstream nodes, b) the number of upstream and downstream branches, and c) the names of the upstream and downstream branches. Figure 5 shows an example of relational properties of a branch in a given network.

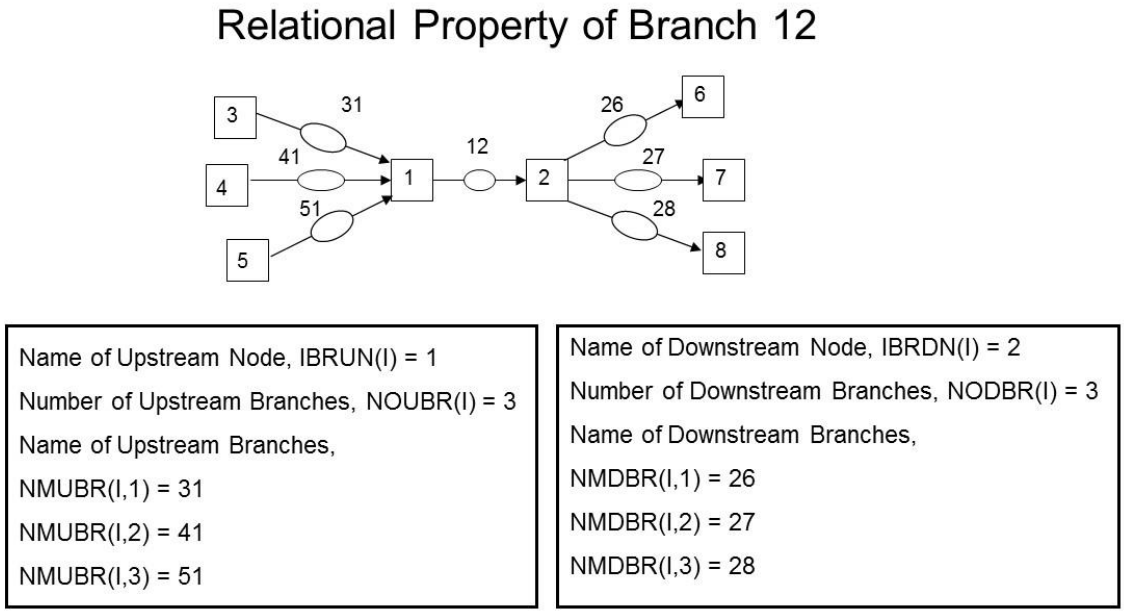

Figure 5. Example of Relational Property of a Branch

2.3 Governing Equations

The flow is assumed to be Newtonian, non-reacting and compressible. It can be steady or unsteady, laminar or turbulent, with or without heat transfer, phase change, mixing or rotation. Figure 6 displays a schematic showing adjacent nodes, their connecting branches, and the indexing system. In order to solve for the unknown variables, mass, energy and fluid species, conservation equations are written for each internal node and flow rate equations are written for each branch.

2.3.1 Mass Conservation Equation

The following is the mass conservation equation:

$$\frac{m_{\tau+\Delta\tau} - m_{\tau}}{\Delta\tau} = -\sum_{j=1}^{j=n} \dot{m}_{ij} \qquad (1)$$

Equation 1 requires that for the unsteady formulation, the net mass flow from a given node must equate to the rate of change of mass in the control volume. In the steady state formulation, the left side of the equation is zero. This implies that the total mass flow rate into a node is equal to the total mass flow rate out of the node.

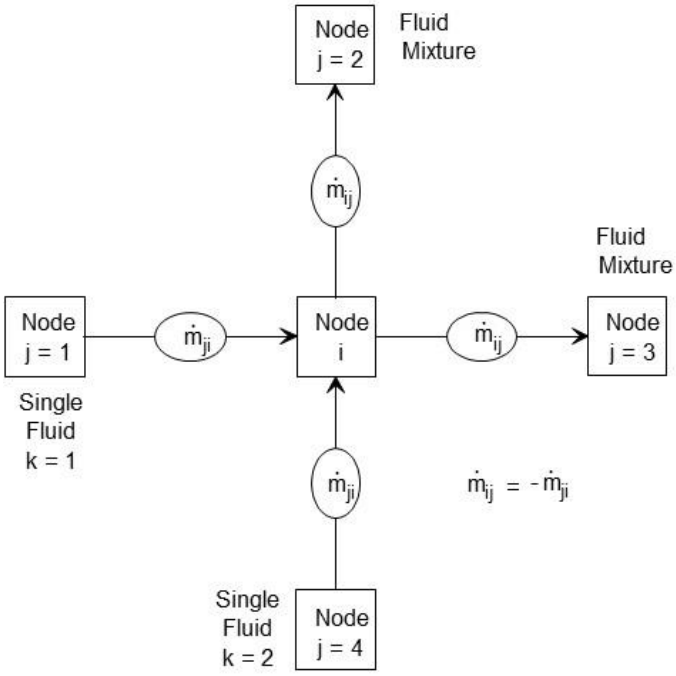

Figure 6. Schematic of Nodes, Branches and Indexing Practice

2.3.2 Momentum Conservation Equation

The flow rate in a branch is calculated from the momentum conservation equation (Equation 2) which represents the balance of fluid forces acting on a given branch. A typical branch configuration is shown in Figure 6. Inertia, pressure, gravity, friction and centrifugal forces are considered in the conservation equation. In addition to these five forces, a source term S has been provided in the equation to input pump characteristics or to input power to a pump in a given branch. If a pump is located in a given branch, all other forces except pressure are zero. The source term, S, is zero in all branches without a pump or other external momentum source.

$$\frac{(mu)_{\tau+\Delta\tau}-(mu)_{\tau}}{g_c\Delta\tau}+MAX\left|\dot{m}_{ij},0\right|\left(u_{ij}-u_u\right)-MAX\left|-\dot{m}_{ij},0\right|\left(u_{ij}-u_u\right)=$$

-- -Unsteady --- ---------- Longitudinal Inertia ----------

$$\left(p_i-p_j\right)A_{ij}+\frac{\rho gVCos\theta}{g_c}-K_f\,\dot{m}_{ij}\left|\dot{m}_{ij}\right|A_{ij}+\frac{\rho K_{rot}^2\omega^2A}{g_c}-\rho A_{norm}u_{norm}u_{ij}/g_c+S \qquad (2)$$

--Pressure -- Gravity -- Friction -- Centrifugal -- Moving Boundary -- Source

Unsteady

This term represents the rate of change of momentum with time. For steady state flow, the time step is set to an arbitrary large value and this term reduces to zero.

Longitudinal Inertia

This term is important for compressible flows when there is a significant change in velocity in the longitudinal direction due to change in area and/or density. An upwind differencing scheme is used to compute the velocity differential.

Pressure

This term represents the pressure gradient in the branch. The pressures are located at the upstream and downstream face of a branch.

Gravity

This term represents the effect of gravity. The gravity vector makes an angle (θ) with the assumed flow direction vector. At $\theta = 180°$ the fluid is flowing against gravity; at $\theta = 90°$ the fluid is flowing horizontally, and gravity has no effect on the flow.

Friction

This term represents the frictional effect. Friction is modeled as a product of K_f, the square of the flow rate, and the area. K_f is a function of the fluid density in the branch and the nature of the flow passage being modeled by the branch. The calculation of K_f for different types of flow passages is described in a later section.

Centrifugal

This term in the momentum equation represents the effect of the centrifugal force. This term will be present only when the branch is rotating as shown in Figure 7. K_{rot} is the factor representing the fluid rotation. K_{rot} is unity when the fluid and the surrounding solid surface rotate with the same speed. This term also requires knowledge of the distances from the axis of rotation between the upstream and downstream faces of the branch.

Moving Boundary

This term represents the force exerted on the control volume by a moving boundary. This term is not active for multi-dimensional calculations.

Source

This term represents a generic source term. Any additional force acting on the control volume can be modeled through the source term. In a system level model, a pump can be modeled by this term. A detailed description of modeling a pump by this source term, S, appears in a later section.

In a system level thermo-fluid model, compressible flow through an orifice is often an option for a branch. Under that circumstance, instead of solving equation 2, a simplified form of momentum equation is solved to calculate flowrate through an orifice. If the ratio of downstream to upstream pressure is less than the critical pressure ratio:

$$\frac{p_j}{p_i} < p_{cr}\,, \qquad \text{(3a)}$$

where:

$$p_{cr} = \left(\frac{2}{\gamma+1}\right)^{\frac{\gamma}{\gamma-1}}\,, \qquad \text{(3b)}$$

then the choked flow rate in the branch is calculated from:

$$\dot{m}_{ij} = C_{L_{ij}} A \sqrt{p_i \rho_i g_c \frac{2\gamma}{\gamma - 1}\left(p_{cr}\right)^{2/\gamma}\left[1 - \left(p_{cr}\right)^{(\gamma-1)/\gamma}\right]}. \qquad (3c)$$

If $\frac{p_j}{p_i} > p_{cr}$ the un-choked flow rate in the branch is calculated from:

$$\dot{m}_{ij} = C_{Lij} A \sqrt{p_i \rho_i g_c \frac{2\gamma}{\gamma - 1}\left(\frac{p_j}{p_i}\right)^{2/\gamma}\left[1 - \left(\frac{p_j}{p_i}\right)^{(\gamma-1)/\gamma}\right]} \qquad (3d)$$

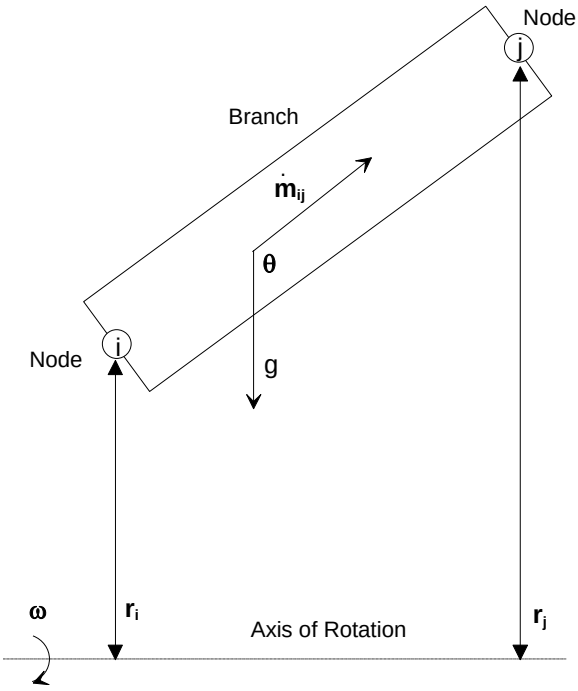

Figure 7 - Schematic of a Branch Showing Gravity and Rotation

2.3.3 Energy Conservation Equations for fluid and solid

Energy Conservation Equation of Fluid

The main purpose of the energy conservation equation in fluid flow calculations is to obtain fluid properties which are primarily functions of pressure and temperature. While pressures are calculated from the mass conservation equation, to obtain temperatures and other properties, the energy equation must be solved. The energy conservation equation can be expressed in terms of enthalpy or entropy. Once pressure and enthalpy or pressure and entropy are known, all thermodynamic and

thermo-physical properties can be evaluated by using the available computer programs [12-14] that calculate properties of common fluids.

The energy conservation equation in terms of enthalpy for node *i*, shown in Figure 6, can be expressed as:

$$\frac{m\left(h-\frac{p}{\rho J}\right)_{\tau+\Delta\tau}-m\left(h-\frac{p}{\rho J}\right)_{\tau}}{\Delta\tau}=$$

$$\sum_{j=1}^{j=n}\left\{MAX\left[-\dot{m}_{ij},0\right]h_j-MAX\left[\dot{m}_{ij},0\right]h_i\right\}+\frac{MAX\left[-\dot{m}_{ij},0\right]}{\left|\dot{m}_{ij}\right|}\left[\left(p_i-p_j\right)+K_{ij}\dot{m}_{ij}^{2}\right]\left(\upsilon_{ij}\mathrm{A}\right)+Q_i \tag{4}$$

Equation 4 shows that for transient flow, the rate of increase of internal energy in the control volume is equal to the rate of energy transport into the control volume minus the rate of energy transport from the control volume plus the rate of work done on the fluid by the pressure force plus the rate of work done on the fluid by the viscous force plus the rate of heat transfer into the control volume. The term $\left(p_i-p_j\right)\nu_{ij}A_{ij}$ represents work input to the fluid due to rotation or having a pump in the upstream branch of the node *i*. The term $K_{ij}\,\dot{m}_{ij}^{2}\,\nu_{ij}A_{ij}$ represents viscous work in the upstream branch of the node *i* where ν_{ij} and A_{ij} are velocity and area of the upstream branch.

The energy conservation equation based on entropy is shown in Equation 5.

$$\frac{(ms)_{\tau+\Delta\tau}-(ms)_{\tau}}{\Delta\tau}=\sum_{j=1}^{j=n}\left\{MAX\left[-\dot{m}_{ij},0\right]s_j-MAX\left[\dot{m}_{ij},0\right]s_i\right\}+\sum_{j=1}^{j=n}\left\{\frac{MAX\left[-\dot{m}_{ij},0\right]}{\left|\dot{m}_{ij}\right|}\right\}\dot{S}ij,gen+\frac{Q_i}{T_i} \tag{5}$$

The entropy generation rate due to fluid friction in a branch is expressed as

$$\dot{S}_{ij,gen}=\frac{\dot{m}_{ij}\,\Delta p_{ij,viscous}}{\rho_u T_u J}=\frac{K_f\left(\left|\dot{m}_{ij}\right|\right)^3}{\rho_u T_u J} \tag{5a}$$

The first term in the right hand side of the equation represents the convective transport of entropy from neighboring nodes. The second term represents the rate of entropy generation in branches connected to the ith node. The third term represents entropy change due to heat transfer.

Energy Conservation Equation of Solid

Typically a solid node can be connected with other solid nodes, fluid nodes, and ambient nodes. Figure 8 shows a typical arrangement where a solid node is connected with other solid nodes, fluid nodes, and ambient nodes. The energy conservation equation for a solid node i can be expressed as:

$$\frac{\partial}{\partial \tau}\left(mC_p T_s^i\right) = \sum_{j_s=1}^{n_{ss}} \dot{q}_{ss} + \sum_{j_f=1}^{n_{sf}} \dot{q}_{sf} + \sum_{j_a=1}^{n_{sa}} \dot{q}_{sa} + \dot{S}_i \qquad (6)$$

The left hand side of the equation represents the rate of change of temperature of the solid node, i. The right hand side of the equation represents the heat transfer from the neighboring node and heat source or sink. The heat transfer from neighboring solid, fluid and ambient nodes can be expressed as

$$\dot{q}_{ss} = k_{ij_s} A_{ij_s} / \delta_{ij_s} \left(T_s^{j_s} - T_s^i\right) \qquad (6a)$$

$$\dot{q}_{sf} = h_{ij_f} A_{ij_f} \left(T_f^{j_f} - T_s^i\right) \qquad (6b)$$

$$\dot{q}_{sa} = h_{ij_a} A_{ij_a} \left(T_a^{j_a} - T_s^i\right) \qquad (6c)$$

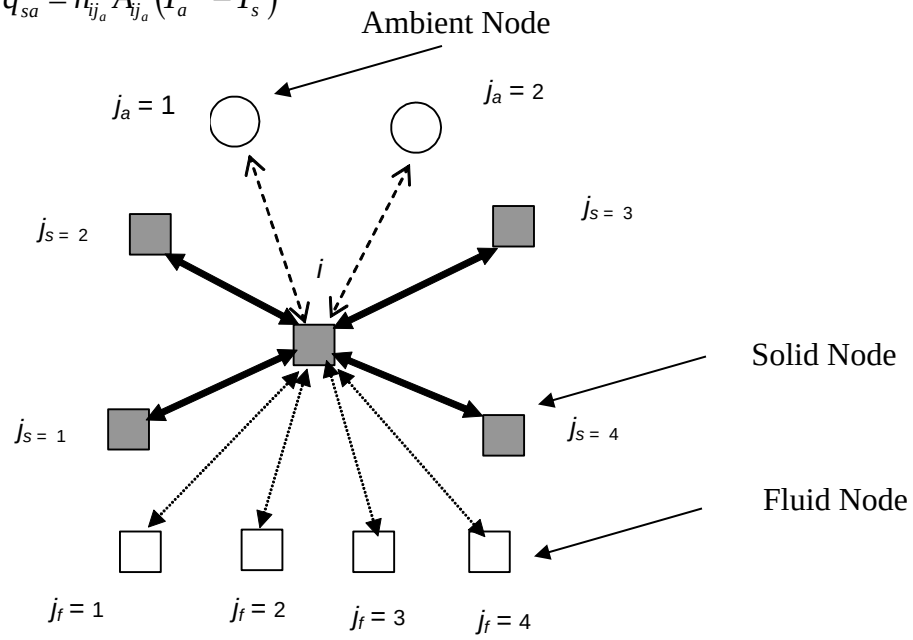

Figure 8. A schematic showing the connection of a solid node with neighboring solid, fluid and ambient nodes

The effective heat transfer coefficients for solid to fluid and solid to ambient nodes are expressed as the sum of the convection and radiation:

$$
\begin{aligned}
h_{ij_f} &= h_{c,ij_f} + h_{r,ij_f} \\
h_{ij_a} &= h_{c,ij_a} + h_{r,ij_a} \\
h_{r,ij_f} &= \frac{\sigma\left[\left(T_f^{j_f}\right)^2 + \left(T_s^i\right)^2\right]\left[T_f^{j_f} + T_s^i\right]}{1/\varepsilon_{ij,f} + 1/\varepsilon_{ij,s} - 1} \\
h_{r,ij_a} &= \frac{\sigma\left[\left(T_a^{j_a}\right)^2 + \left(T_s^i\right)^2\right]\left[T_a^{j_a} + T_s^i\right]}{1/\varepsilon_{ij,a} + 1/\varepsilon_{ij,s} - 1}
\end{aligned}
\tag{6d}
$$

2.3.4 Equation of State and Thermodynamic Properties

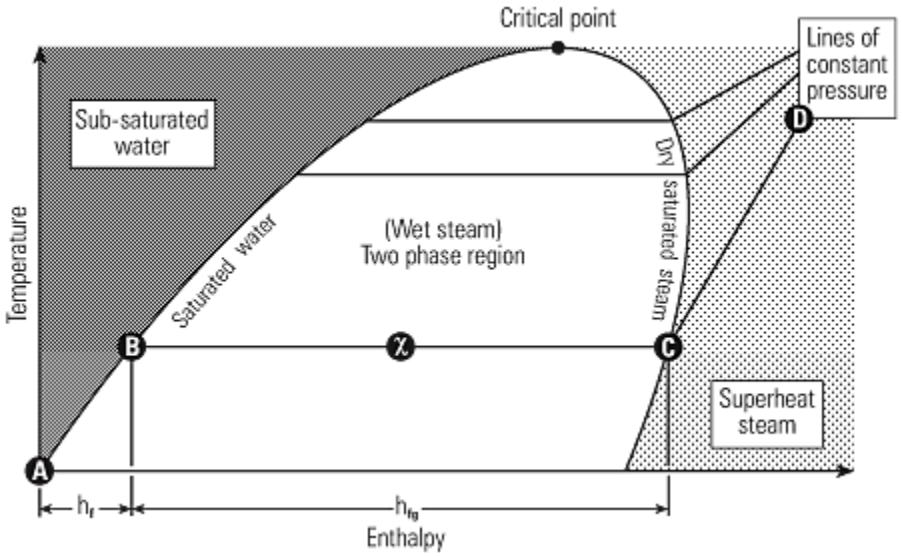

Figure 9. Thermodynamic state of a real fluid

The conservation equations for mass, momentum and energy contain thermodynamic and thermo-physical properties of a real fluid. A real fluid can exist in different states as shown in Figure 9: subcooled liquid (A), saturated liquid (B), a mixture of liquid and vapor (x), saturated vapor (C), and superheated vapor (D). The state of the real fluid in a given node is calculated from its pressure and enthalpy using a thermodynamic property program such as GASP [12] or GASPAK [14]. All these programs use accurate equations of state for thermodynamic properties and correlations for thermo-physical properties for common fluids.

One of the main objectives of using an accurate equation of state is to compute the compressibility factor z, which is used in the equation of state to compute the resident mass of the node:

$$m = \frac{pV}{RTz} \tag{7}$$

2.3.5 Species Conservation Equation

For a fluid mixture, thermodynamic and thermo-physical properties are also a function of the mass fraction of the fluid species. In order to calculate the properties of the mixture, the concentration of the individual fluid species within the branch must be determined. The concentration for the k[th] species can be written as

$$\frac{\left(m_i c_{i,k}\right)_{\tau+\Delta\tau} - \left(m_i c_{i,k}\right)_{\tau}}{\Delta\tau} = \sum_{j=1}^{j=n} \left\{ MAX\left[-\dot{m}_{ij}, 0 \right] c_{j,k} - MAX\left[\dot{m}_{ij}, 0 \right] c_{i,k} \right\} + \dot{S}_{i,k} \tag{8}$$

For transient flow, Equation 8 states that the rate of increase of the concentration of the k[th] species in the control volume equals the rate of transport of the k[th] species into the control volume minus the rate of transport of the k[th] species out of the control volume plus the generation rate of the k[th] species in the control volume.

2.3.6 Mixture Properties

A homogeneous mixture of multiple species in a given network can also be modeled provided the properties of the mixture are computed from the properties of the component species.

Temperature

In the absence of phase change, the temperature of the node can be calculated from a modified energy equation which is expressed in terms of specific heat and temperature.

$$\left(T_i\right)_{\tau+\Delta\tau} = \frac{\sum_{j=1}^{j=n} \sum_{k=1}^{k=nf} \mathrm{Cp}_{k,j} x_{k,j} T_j MAX\left[-\dot{m}_{ij}, 0 \right] + \left(C_{p,i} m_i T_i\right)_{\tau} / \Delta\tau + Q_i}{\sum_{j=1}^{j=n} \sum_{k=1}^{k=nf} \mathrm{Cp}_{k,j} x_{k,j} MAX\left[\dot{m}_{ij}, 0 \right] + \left(C_{p,i} m\right)_{\tau+\Delta\tau} / \Delta\tau} \tag{9}$$

Density

For Amagat's model of partial volume, mixture density is expressed as:

$$\frac{1}{\rho_{mix}} = \sum \frac{x_k}{\rho_k} \tag{10}$$

ρ_k is evaluated at node pressure, p_i.

For Dalton's model of partial pressures, mixture density is expressed as:

$$\rho_{mix} = \sum \rho_k \tag{11}$$

ρ_k is evaluated at partial pressure, p_k. which is product of molar concentration and node pressure, p_i.

Compressibility Factor

The compressibility factor of the mixture, z_i is expressed as

$$z_i = \sum_{k=1}^{k=n} x_k z_k \tag{12}$$

where

$$z_k = \frac{p_i}{\rho_k R_k T_i} \tag{12a}$$

2.3.7 Friction Calculation

It was mentioned earlier that the friction term in the momentum equation is expressed as a product of K_f, the square of the flow rate, and the flow area. Empirical information is necessary to estimate K_f . For pipe flow (Figure 10), length, *L*, diameter, *D*, and surface roughness, ε are needed to compute friction.

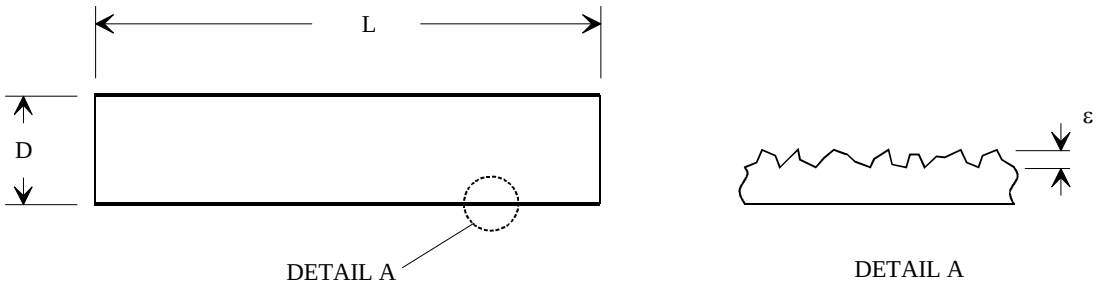

Where:
D = Pipe Diameter
L = Pipe Length
ε = Absolute Roughness

Figure 10 - Pipe parameters to compute friction

K_f can be expressed as:

$$K_f = \frac{8fL}{\rho_u \pi^2 D^5 g_c} \tag{13}$$

The Darcy friction factor, f, is determined from the Colebrook Equation [8] which is expressed as:

$$\frac{1}{\sqrt{f}} = -2\log\left[\frac{\varepsilon}{3.7D} + \frac{2.51}{\mathrm{Re}\sqrt{f}}\right] \qquad (13a)$$

To compute friction in a flow through a restriction with a given flow coefficient, C_L, and area, A, K_f can be expressed as:

$$K_f = \frac{1}{2 g_c \rho_u C_L^2 A^2} \qquad (14)$$

In classical fluid mechanics, head loss is expressed in terms of a non-dimensional "K factor".

$$\Delta h = K\frac{u^2}{2g} \qquad (14a)$$

K and C_L are related as:

$$C_L = \frac{1}{\sqrt{K}} \qquad (14b)$$

Reference [10] describes the friction calculations of other fluid components such as valve, bend and orifice.

2.3.8 Heat Transfer Coefficient

The heat transfer coefficient is necessary to calculate heat transfer between solid to fluid (Equation 6b). The heat transfer coefficient is determined from empirical correlations.

There are four different options for specifying the heat transfer coefficient:

1. A constant heat transfer coefficient
2. The Dittus-Boelter equation [Equation 15] for single phase flow where Nusselt number is expressed as:

$$\frac{h_c D}{k_f} = 0.023\left(\mathrm{Re}\right)^{0.8}\left(\mathrm{Pr}\right)^{0.33} \qquad (15)$$

where $\mathrm{Re} = \dfrac{\rho u D}{\mu_f}$ and $\mathrm{Pr} = \dfrac{C_p \mu_f}{k_f}$

3. Miropolsky's correlation [29] for two phase flow

$$Nu = 0.023\left(\mathrm{Re}_{mix}\right)^{0.8}\left(\mathrm{Pr}_v\right)^{0.4}\left(Y\right) \qquad (16)$$

$$\mathrm{Re}_{mix} = \left(\frac{\rho u D}{\mu_v}\right)\left[x + \left(\frac{\rho_v}{\rho_l}\right)(1-x)\right]$$

$$\mathrm{Pr}_v = \left(\frac{C_p \mu_v}{k_v}\right)$$

$$Y = 1 - 0.1\left(\frac{\rho_l}{\rho_v} - 1\right)^{0.4}(1-x)^{0.4}$$

4. A new, user-defined correlation can be implemented in the User Subroutine described in Section 4.

2.4 Closure

The purpose of the mathematical formulation was to describe the governing equations to solve for the necessary variables of a given thermo-fluid network. The mathematical closure is shown in Table 1 where each variable and the designated governing equation to solve that variable are listed.

Table 1 – Mathematical Closure

Variable Name	Designated Equation to Solve the Variable
Pressure	Mass Conservation (Eqn. 1)
Flowrate	Momentum Conservation (Eqn. 2)
Fluid Enthalpy or Entropy	Energy Conservation of Fluid (Eqn. 4 & 5)
Solid Temperature	Energy Conservation of Solid (Eqn. 6)
Species Concentration	Species Conservation (Eqn. 8)
Fluid Mass	Thermodynamic State (Eqn. 7)

It may be noted that the pressure is calculated from the mass conservation equation although pressure does not explicitly appear in equation 1. This is, however, possible in the iterative Newton-Raphson scheme where pressures are corrected to reduce the residual error in the mass conservation equation. This practice was first implemented in the SIMPLE (Semi-Implicit Pressure Linked Equation) algorithm proposed by Patankar and Spalding [4] and commonly referred to as a "Pressure Based" algorithm in Computational Fluid Dynamics literature. The momentum conservation equation (equation 2), which contains both pressure and flowrate, is solved to calculate the flowrate. The strong coupling of pressure and flowrate requires that the mass and momentum conservation equations be solved simultaneously. In the following section, the numerical method of solving the system of equations listed in Table 1, will be described.

3. Numerical Method

A fully implicit iterative numerical method has been used to solve the system of equations described in the previous section. There are two types of numerical methods available to solve a set of non-linear coupled algebraic equations: (1) the Successive Substitution method and (2) the Newton-Raphson method. In the Successive Substitution method, each

equation is expressed explicitly to calculate one variable. The previously calculated variable is then substituted into the other equations to calculate another variable. In one iterative cycle each equation is visited. The iterative cycle is continued until the difference in the values of the variables in successive iterations becomes negligible. The advantages of the Successive Substitution method are its simplicity to program and its low code overhead. The main limitation, however, is finding the optimum order for visiting each equation in the model. This visiting order, which is called the information flow diagram, is crucial for convergence. Under-relaxation (partial substitution) of variables is often required to obtain numerical stability.

In the Newton-Raphson method, the simultaneous solution of a set of non-linear equations is achieved through an iterative guess and correction procedure. Instead of solving for the variables directly, correction equations are constructed for all of the variables. The intent of the correction equations is to eliminate the error in each equation. The correction equations are constructed in two steps: (1) the residual errors in all of the equations are estimated and (2) the partial derivatives of all of the equations, with respect to each variable, are calculated. The correction equations are then solved by the Gaussian elimination method. These corrections are then applied to each variable, which completes one iteration cycle. These iterative cycles of calculations are repeated until the residual error in all of the equations is reduced to a specified limit. The Newton-Raphson method does not require an information flow diagram. Therefore, it has improved convergence characteristics. The main limitation to the Newton-Raphson method is its requirement for a large amount of computer memory.

In the present finite volume procedure, a combination of the Successive Substitution method and the Newton-Raphson method is used to solve the set of equations. This method is called SASS (Simultaneous Adjustment with Successive Substitution). In this scheme, the mass and momentum conservation equations are solved by the Newton-Raphson method. The energy and species conservation equations are solved by the Successive Substitution method. The underlying principle for making such a division was that the equations that are more strongly coupled are solved by the Newton-Raphson method. The equations that are not strongly coupled with the other set of equations are solved by the Successive Substitution method. Thus, the computer memory requirement can be significantly reduced while maintaining superior numerical convergence characteristics. Figure 11 shows the flow chart of the numerical scheme.

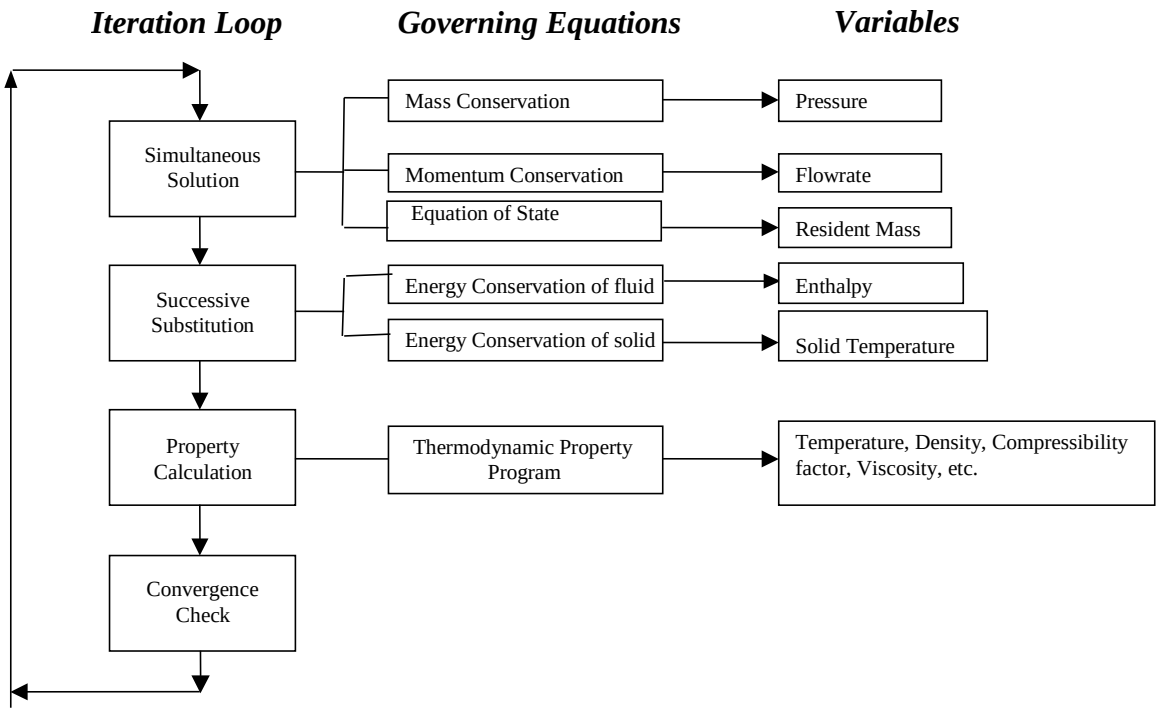

Figure 11. SASS (Simultaneous Adjustment with Successive Substitution) Scheme for solving Governing Equations

4. Computer Program

This numerical method has been incorporated into a general-purpose computer program, GFSSP [9-11]. There are seven major functions of the computer program:

1. Development of a flow circuit of fluid and solid nodes with branches and conductors
2. Development of an indexing system or data structure to define a network of fluid and solid nodes with branches and conductors
3. Generation of the conservation equations of mass, momentum, energy, species concentration, and solid temperatures in respective nodes and branches
4. Calculation of the thermodynamic and thermo-physical properties of the fluid and solid in nodes
5. Numerical solution of the conservation equations
6. Input / Output
7. User-Defined Modules.

GFSSP consists of three major modules: the Graphical User Interface (GUI), the Solver and Property module, and the User Subroutine module. Figure 12 shows the process flow diagram to describe the interaction among the three modules. A flow circuit is created in the GUI by a "point, drag and click" method and an input data file is created which is read by the Solver and Property module. Specialized input to the model can be applied through a User Subroutine. Such specialized input includes time dependent processes; non-linear boundary conditions; external mass, momentum and energy sources; customized output;

and new resistance and fluid options. More details of the computer program are provided in Reference [10].

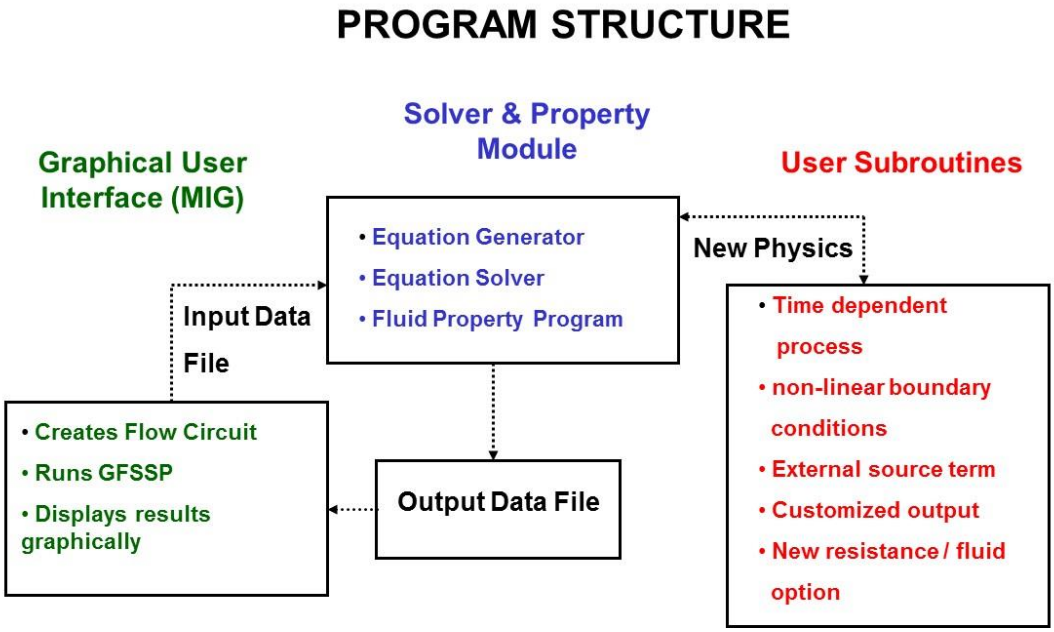

Figure 12. Process Flow Diagram showing interaction among three modules

5. Applications

The development of this method started in 1994. Since then the described finite volume method for network flow analysis has been successfully applied to simulate a large number of aerospace applications, namely (a) internal flow in a rocket engine turbo-pump, (b) compressible flows in ducts and nozzles, (c) pressurization and loading of a cryogenic propellant tank, (d) fluid transient during sudden opening of a valve for priming of partially evacuated propellant feed line, and (e) chilldown of a cryogenic transfer line with phase change and two phase flows.

5.1 Flow in a Rocket Engine Turbopump

In this rocket engine turbopump, a turbine, driven by hot gas from a gas generator, drives two pumps for pumping liquid fuel and oxygen before they are ignited in the thrust chamber. Both turbine and pumps are mounted on the same shaft which rotates around 30,000 rpm. There are many design challenges for a successful operation of this complex machine. Network analysis is particularly useful to a) estimate the axial load on the bearings, b) ensure appropriate flow through the bearings for cooling, and c) design the inter-propellant seal to prevent any mixing of fuel and oxidizer in the turbopump. References 15 and 16 describe the network flow analysis of internal flow in a rocket engine pump to address the above mentioned design issues. The numerical predictions of pressure and temperature at various locations in the turbopump compare well with experimental data.

5.2 Compressible flows in ducts and nozzles

The capability to model tank blowdown and flow through a converging-diverging nozzle was demonstrated in reference 10 by comparing numerical predictions with analytical solutions. Reference 17 presents a numerical study of the effect of friction, heat transfer and area change in subsonic compressible flow. The numerical solutions of pressure, temperature and Mach number have been compared with benchmark solutions for different cases representing the effect of friction, heat transfer and area change.

5.3 Modeling of a Cryogenic Tank

Modeling of a cryogenic tank is important for the design of liquid propulsion systems. In a liquid propulsion system, cryogenic tanks are subjected to different processes which must be modelled to ensure all fluid properties are within the margin of safe and reliable operation. A robust and accurate network flow analysis method is necessary to simulate processes such as Tank Loading, Boil-off and Tank Pressurization.

Tank Loading

One of the very first and longest ground operations before a rocket launch is the loading of cryogenic propellants from the ground storage tanks into the launch vehicle tanks. This process takes several hours because the cryogenic transfer lines and propellant tanks must be chilled down from ambient temperature to liquid propellant temperatures, approximately 20 K for liquid hydrogen (LH2) and 90 K for liquid oxygen (LO2). The primary source of this cooling is the latent heat of vaporization: when cryogenic propellants are introduced into the transfer lines and vehicle tanks, they extract energy from the pipe and tank walls and evaporate. The vaporized propellants are vented from the vehicle tank, either to a flare stack, in the case of hydrogen, or to the atmosphere, in the case of oxygen. A numerical model was developed [18] to model the loading of liquid hydrogen and oxygen in the external tank of the Space Shuttle from storage tanks which are quarter-mile away from the launch site. The model predictions compared well with measured data.

The practice of tank loading in a micro-gravity environment is quite different from tank loading on the ground. On the ground, under normal gravity, a vent valve on top of the tank can be kept open to vent the vapor generated during the loading process. The tank pressure can be kept close to atmospheric pressure while the tank is chilling down. In a micro-gravity environment, due to the absence of stratification, such practice may result in dumping large amount of precious liquid propellant overboard. The intent of the no-vent chill and fill method is to minimize the loss of propellant during chilldown of a propellant tank in a micro-gravity environment. The no-vent chill and fill method consists of a repeated cyclic process of charge, hold and vent. A numerical model was developed [19] to simulate chilldown of an LH2 tank at the K-site Test Facility at NASA/Glenn Research Center and numerical predictions were compared with test data.

Boil-off of Cryogenic Propellants

The cost of loss of propellants due to boil-off in large cryogenic storage tanks is on the order of one million dollars per year. One way to reduce this cost is to design a new tank or refurbish existing tanks by using bulk-fill insulation material with improved thermal performance. An accurate numerical model of the boil-off process can help to design a tank with improved boil-off performance. A numerical model of the boil-off in a cryogenic storage tank at NASA's Kennedy Space Center was developed [20]. The model developments were carried out in two phases. First, the model was verified with test data from a Demonstration Tank using liquid nitrogen and hydrogen. The verified model was then extended to model the full-scale storage tank and the predictions were compared with field data.

Tank Pressurization

In a liquid propulsion system cryogenic propellants are stored in an insulated tank. The propellants from the tank are fed to the turbo-pump by pressurizing the tank by an inert gas such as helium. The tank pressures must be controlled within a certain band for reliable operation of the turbo-pump. The pressurization of a propellant tank is a complex thermodynamic process with heat and mass transfer in a stratified environment. Numerical prediction of the pressurization process was compared [21] with correlations derived from test data. The agreement between the predictions and correlations was found to be satisfactory. The numerical model developed in reference [21] was extended to model the helium pressurization system of a Propulsion Test Article at NASA/Stennis Space Center where NASA's Fastrac engine [15] was tested. A detailed numerical model [22] of the Tank Pressurization system was developed. The model included a helium feed line, control valves, liquid oxygen and RP-1 (Kerosene) tanks, and liquid oxygen and RP-1 feedlines supplying the propellants to the engine. The control valves of both tanks were modeled to set the pressure within a specified band. The model also accounted for the heat transfer between the helium and propellants and between the helium and the tank wall in the ullage, which is the gaseous space in the tank. The predicted pressure in both tanks compared well with test data.

In long duration space travel, the cryogenic propellant tanks are self-pressurized due to heat transfer from space to the tank. The ullage pressure is controlled by the Thermodynamic Vent System (TVS). A TVS typically includes a Joule-Thompson expansion devise, a two-phase heat exchanger, a mixing pump and a liquid injector to extract thermal energy from the tank without significant loss of liquid propellant. A numerical model of a system level test bed was developed [23] to simulate self-pressurization and pressure control by a TVS. The numerical prediction compared reasonably well with experimental data,

5.4 Fluid transient due to sudden opening of a valve

Fluid transient due to sudden opening of a valve is important in propulsion applications when propellant valves are instantaneously opened to feed the thrusters with fuel and oxidizer. The pressure rise could be of the order of two hundred atmosphere (20 MPa). Designers need to have an analytical tool to estimate the maximum pressure and frequency of oscillation to ensure the structural integrity of the propulsion system. A laboratory experiment was performed [24] with water and air to measure the pressure oscillation following a sudden closure of a valve. An 11-meter pipe (2.6 centimeter in diameter) was connected to a water tank at one end and closed at the other end. A valve was placed 6 meters from the tank. The valve was initially closed and air at atmospheric pressure was entrapped downstream of the valve. The pressure in the tank was varied from 203 kPa to 710 kPa. This experimental configuration was first modeled [25] assuming a lumped air node with a variable volume. Only the thermodynamics of the air were modeled; the air was considered stagnant. The numerical predictions of pressure oscillation compared well with measurements. Later a more detailed model of the air-water system was developed and is shown in Figure 13. In this model, the pipe containing air was also modeled and discretized with several nodes and branches similar to the pipe containing water upstream of the valve. After the opening of the valve, air and water mix, and water penetrates into the air and pushes the air towards the dead end. Boundary Node 1 represents the tank, and the restriction in branch 1112 indicates the ball valve. The history of the ball valve opening is shown in Figure 14.

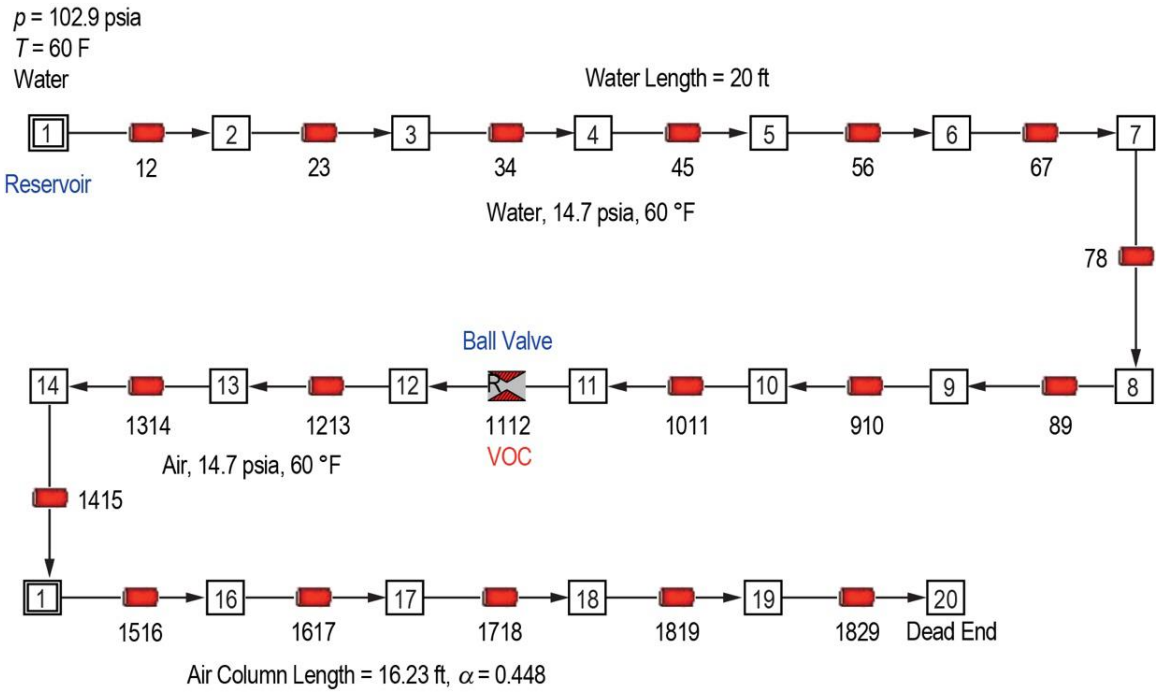

Figure 13. Computational Model of Lee's [24] experimental set up.

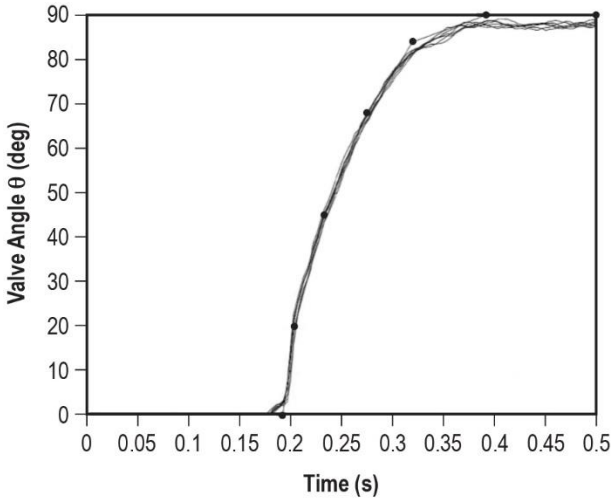

Fig.14. Ball valve angle change with time [].

The comparison between numerical predictions and experimental data is shown in Figure 15. The frequency of oscillation matches quite well with test data. However, the numerical model predicts a higher peak pressure than test data. The cause of this discrepancy can be attributed to the assumption of a rigid pipe. The experiments were performed in Plexiglas pipe and the elastic deformation of the pipe could be the cause of lower peak pressure in the experiments. More applications and verifications of this procedure are described in Reference [26].

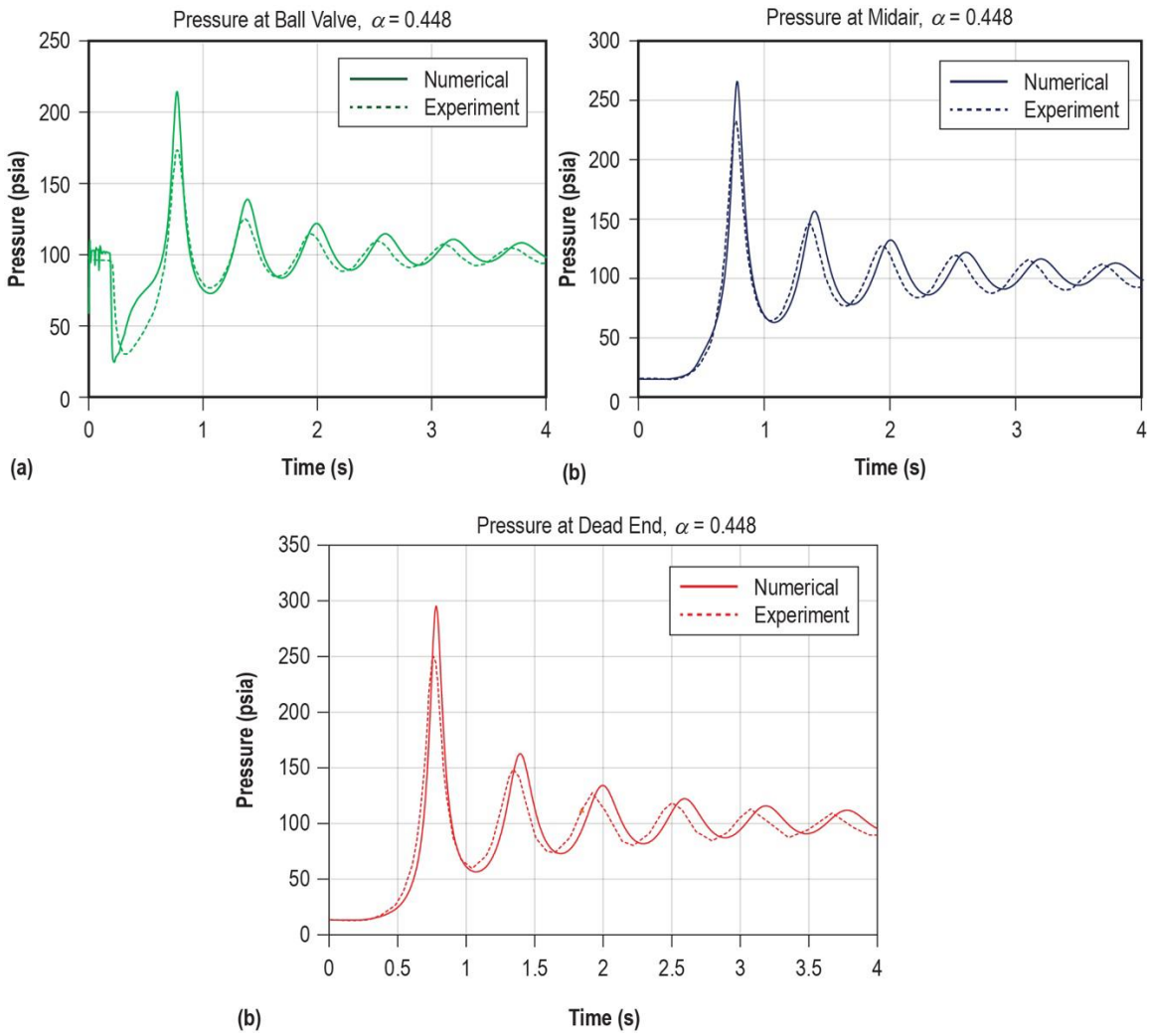

Figure 15. Comparison between numerical predictions and measured data at (a) Ball Valve, (b) mid-section, and, (c) dead end for $P_R = 7$, and $\alpha = 0.448$

5.5 Chilldown of a transfer line carrying cryogenic fluid

A cryogenic transfer line must be chilled down to cryogenic temperature before steady flowrates can be achieved to engine feed or tank-to-tank propellant transfer. A numerical model of the chilldown process is useful for optimizing for time to chilldown or minimum loss of useful propellants. Cross et al [27] first applied the present numerical scheme to model chilldown of a cryogenic transfer line. The numerical prediction was compared with an analytical solution to verify the accuracy of the numerical scheme. The verification and validation of the finite volume procedure for the prediction of conjugate heat transfer in a fluid network was performed by comparing the predictions with available experimental results for a long cryogenic transfer line model reported in [28]. The experimental setup consists of a 200-ft long, 0.625-in-inside diameter copper tube supplied by a 300-L tank through a valve and exits to the atmosphere (≈12.05 psia). The

tank was filled either with LH2 or LN2. At time zero, the valve at the left end of the pipe was opened, allowing liquid from the tank to flow into the ambient pipeline driven by tank pressure.

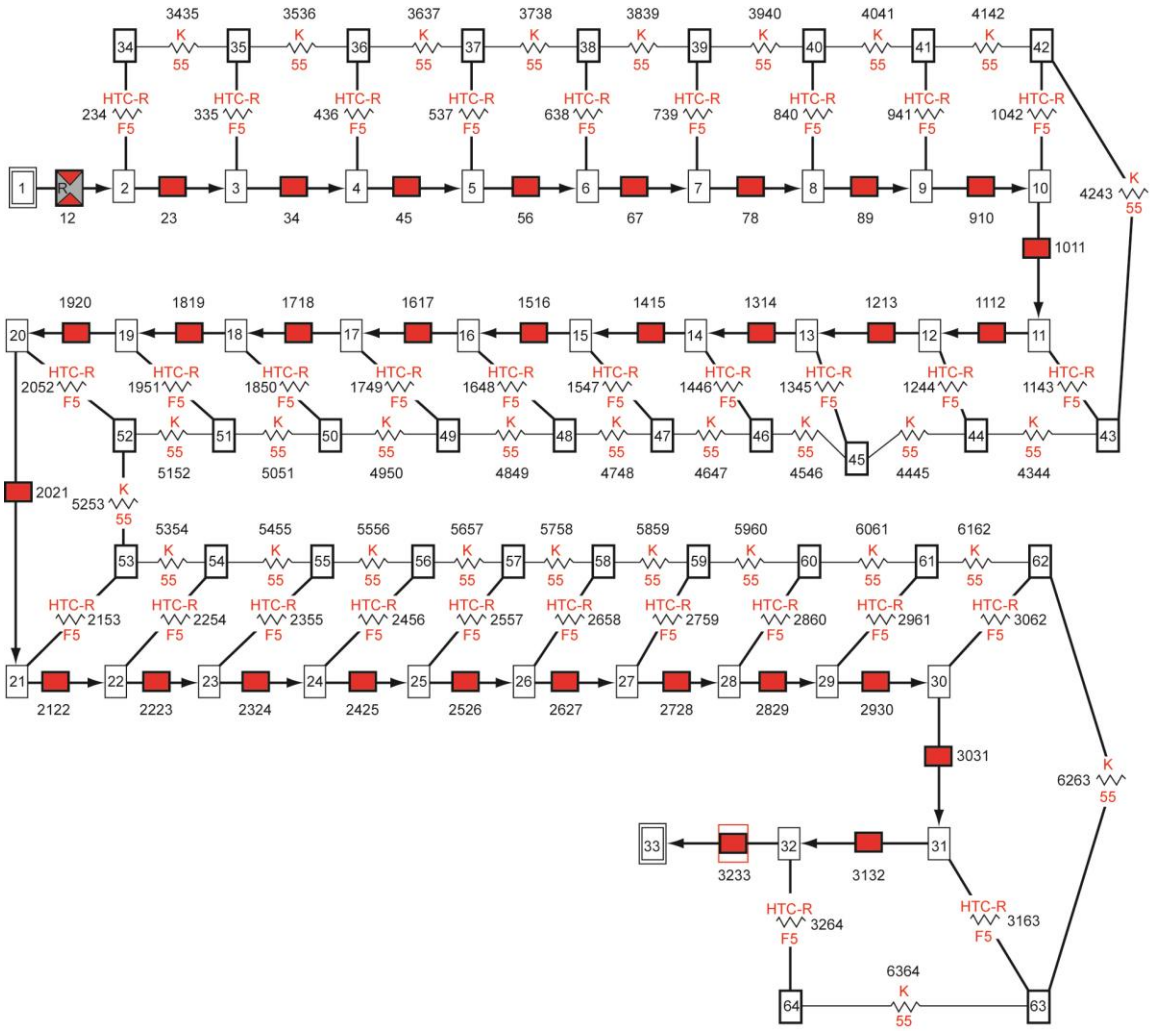

Fig. 16 Network flow model of the fluid system consisting of a tank, pipeline, and valve constructed with boundary nodes, internal nodes, and branches.

Figure 16 shows a schematic of the network flow model that was constructed to simulate the cooling of the transfer line. The tube was discretized into 33 fluid nodes (two boundary nodes and 31 internal nodes), 31 solid nodes, and 32 branch nodes. The upstream boundary node represents the cryogenic tank, while the downstream boundary node represents the ambient where the fluid is discharged. The first branch represents the valve; the next 30 branches represent the transfer line. Each internal node was connected to a solid node (nodes 34 through 64) by a solid to fluid conductor. The heat transfer in the wall is modeled using the lumped parameter method, assuming the wall radial temperature gradient is small. The heat transfer coefficient of the energy equation for the

solid node was computed from the Miropolsky correlation [29]. The experimental work reported in [30] did not provide details concerning the flow characteristics for the valve used, nor did they give a history of the valve opening times that they used. An arbitrary 0.05-s transient opening of the valve was used while assuming a linear change in flow area. The measured and predicted chilldown time for LH_2 and LN_2 chilldown at various pressures at saturated and subcooled conditions are shown in Table 2. It may be noted that at higher pressure it takes less time to chill down. This is primarily due to increased flowrates at higher inlet pressures. In this experimental program [30], however, flowrates were not measured. The effect of subcooling is not significant for LH_2 , but significant for LN_2. Generally numerical models predicted slightly higher chilldown time than measurements. This discrepancy can be attributed to the inaccuracy of the heat transfer coefficient correlation.

Darr et al [31] developed correlations for the entire boiling curve based on a large number of chilldown experiments of a short stainless tube, 0.6 meter long with an inner diameter of 1.17 centimeter, placed inside a vacuum chamber to minimize parasitic heat leak. Flowrates were also measured in addition to temperature history in upstream and downstream locations of the tube. LeClair et al [32], however, found that the Miropolsky correlation was not adequate for a short tube using LN_2 and used this new correlation. The comparison of numerical predictions with experimental data for five different Reynolds numbers is shown in Figure 17.

Table 2. Chilldown time for various driving pressures and temperatures for LH_2 and LN_2

Fluid	Driving Pressure (MPa)	Inlet State	Inlet Temperature (K)	Experimental Chilldown Time (Sec)	Predicted Chilldown Time (Sec)
LH_2	0.52	Saturated	27	68	70
LH_2	0.60	Saturated	28.11	62	69
LH_2	0.77	Saturated	29.6	42	50
LH_2	1.12	Saturated	31.97	30	33
LH_2	0.25	Saturated	19.5	148	150
LH_2	0.43	Subcooled	19.5	75	80
LH_2	0.60	Subcooled	19.5	62	60
LH_2	0.77	Subcooled	19.5	41	45
LH_2	0.94	Subcooled	19.5	32	35
LH_2	1.12	Subcooled	19.5	28	30
LN_2	0.43	Saturated	91.98	165	185
LN_2	0.52	Saturated	94.42	150	160
LN_2	0.60	Saturated	96.35	130	140
LN_2	0.25	Subcooled	76.00	222	250
LN_2	0.34	Subcooled	76.00	170	175
LN_2	0.43	Subcooled	76.00	129	140
LN_2	0.52	Subcooled	76.00	100	100
LN_2	0.60	Subcooled	76.00	85	90

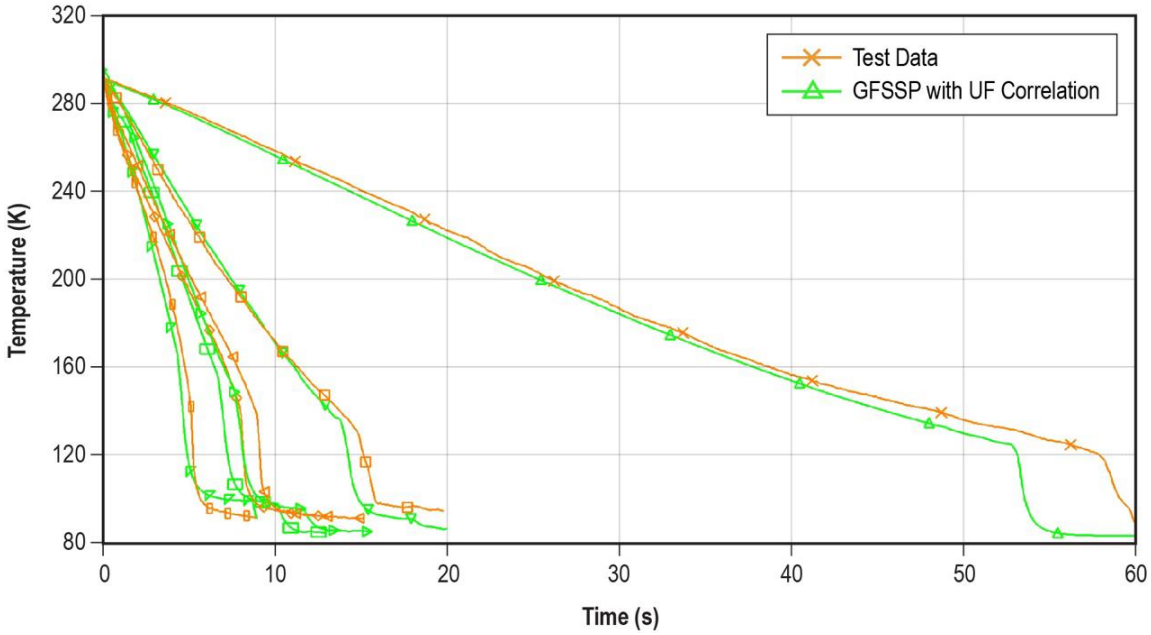

Fig. 17 Downstream wall temperature (K) vs. time (s) for vertical upward LN2 chilldown runs

6. Summary

A finite volume procedure originally developed for solving the Navier-Stokes equation has been implemented in solving the mass, momentum and energy conservation equations in a flow network consisting of various fluid components. The one-dimensional momentum equation is solved in fluid components such as pipes, restrictions, pumps and valves. Fluid friction is calculated using empirical correlations such as friction factor for pipe flows and flow coefficients for orifices and valves. Fluid friction appears as a sink term in the momentum equation. Pumps, on the other hand, are modeled as a source term in the momentum equation, which is calculated from pump characteristics or pump horsepower. Mixtures of species and/or phases are assumed homogeneous. Mass or mole averaged properties of the mixture appear in the conservation equations for mass, momentum and energy. All conservation equations are written in fully implicit form. The mass and momentum conservation equations, as well as the equation of state, are solved simultaneously by the Newton-Raphson method while the energy conservation equations for solid and fluid, and the species conservation equation, are solved by the successive substitution method outside the Newton-Raphson loop. The thermodynamic property calculations are also done outside the Newton-Raphson loop. This method has been successfully applied to several aerospace applications, namely (a) internal flow in a rocket engine turbo-pump, (b) subsonic compressible flows in ducts and nozzles, (c) pressurization and loading of a cryogenic propellant tank, (d) fluid transient during the sudden opening of a valve for priming of a partially evacuated propellant feed line, and (e) chilldown of a cryogenic transfer line with phase change and two phase flows.

7. Acknowledgement

This paper is dedicated to the memory of Professor D. B. Spalding who inspired and guided the author to develop understanding and expertise in the fascinating field of computational thermo-fluid dynamics and heat transfer. The author wants to acknowledge NASA/Marshall Space Flight Center for the opportunity and resources for the continuous development of GFSSP for the last twenty five years. The author also wants to appreciate the contribution and support of Dr. Andre LeClair and other members of the GFSSP development team.

8. References

1. Streeter, V.L., “Fluid Mechanics”, 3rd Edition, McGraw-Hill, 1962.
2. A.D. Gosman, W.M. Pun, A.K. Runchal, D.B.Spalding, M,Wolfshtein , “Heat and Mass Transfer in Recirculating Flows”, Academic Press, 1969
3. Burggraf, O.R.: “Analytical and Numerical Studies of the Structure of Steady Separated Flows”, Journal of Fluid Mechanics, Vol. 24, part 1, pp. 113-151, 1966.
4. Patankar, S.V., and Spalding, D.B.,”A Calculation Procedure for Heat, Mass and Momentum Transfer in Three Dimensional Parabolic Flows,” International Journal of Heat and Mass Transfer, Vol. 15, 1972,pp 1787-1806

5. Launder,B.E., and Spalding, D. B..”The Numerical Computation of Turbulent Flows”,Computer Methods in Applied Mechanics & Engineering, Vol.3, 1974,pp 269-289
6. Majumdar, A. K., "Mathematical Modeling of Flows in Dividing and Combining Flow Manifold," *Applied Mathematical Modeling*, Volume 4, December 1980, pp. 424-431.
7. Datta, A. B. and Majumdar, A. K., "Flow Distribution in Parallel and Reverse Flow Manifolds," *Int. J. Heat and Fluid Flow*, Volume 2, No. 4, 1980.
8. Colebrook, C. F., ”Turbulent Flow in Pipes, with Particular Reference to the Transition Between the Smooth and Rough Pipe Laws”, J. Inst. Civil Engineering, London, vol. 11, pp. 133-156, 1938-1939.
9. Generalized Fluid System Simulation Program - Majumdar; Alok Kumar, Bailey; John W. ; Schallhorn; Paul Alan ; Steadman; Todd E. , United States Patent No. *6,748,349*, June 8, 2004
10. Majumdar AK, LeClair AC, Moore R, Schallhorn PA. Generalized Fluid System Simulation Program, Version 6.0. NASA/TM—2013–217492; October 2013.
11. Majumdar, A. K., “A Second Law Based Unstructured Finite Volume Procedure for Generalized Flow Simulation”, Paper No. AIAA 99-0934, 37th AIAA Aerospace Sciences Meeting Conference and Exhibit, January 11-14, 1999, Reno, NV.
12. Hendricks, R. C., Baron, A. K., and Peller, I. C., “GASP - A Computer Code for Calculating the Thermodynamic and Transport Properties for Ten Fluids: Parahydrogen, Helium, Neon, Methane, Nitrogen, Carbon Monoxide, Oxygen, Fluorine, Argon, and Carbon Dioxide”, NASA TN D-7808, February, 1975.
13. Hendricks, R. C., Peller, I. C., and Baron, A. K., “WASP - A Flexible Fortran IV Computer Code for Calculating Water and Steam Properties”, NASA TN D-7391, November, 1973.
14. Cryodata Inc., “User's Guide to GASPAK, Version 3.20”, November 1994.
15. Van Hooser, Katherine, Majumdar, Alok, Bailey, John, “Numerical Prediction of Transient Axial Thrust and Internal Flows in a Rocket Engine Turbopump” Paper No. AIAA 99-2189, 35th AIAA/ASME/SAE/ASEE, Joint Propulsion Conference and Exhibit, June 21, 1999, Los Angeles, CA.
16. Schallhorn, Paul, Majumdar, Alok, Van Hooser, Katherine and Marsh, Matthew, “Flow Simulation in Secondary Flow Passages of a Rocket Engine Turbopump”, Paper No. AIAA 98-3684, 34th AIAA/ASME/SAE/ASEE, Joint Propulsion Conference and Exhibit, July 13-15, 1998, Cleveland, OH.
17. Bandyopadhyay, Alak and Majumdar, Alok,” Modeling of Compressible Flow with Friction and Heat Transfer using the Generalized Fluid System Simulation Program (GFSSP)” Paper presented in Thermal Fluid Analysis Workshop, NASA Glenn Research Center, September 10-14, 2007
18. LeClair, Andre and Majumdar, Alok,” Computational Model of the Chilldown and Propellant Loading of the Space Shuttle External Tank”, Presented in AIAA Joint Propulsion Conference, Nashville, Tennessee, July, 2010
19. Majumdar, Alok,” No Vent Tank Fill and Transfer Line Chilldown Analysis by GFSSP”, Paper presented in Thermal Fluid Analysis Workshop, NASA Kennedy Space Research Center, July 29 –August 2, 2013

20. Majumdar, A.K. Steadman T.E., Maroney J.L., Sass J.P. and Fesmire J.E.," Numerical Modeling of Propellant Boil-off in a Cryogenic Storage Tank", Cryogenic Engineering Conference, Chattanooga, Tennessee, July 16-20, 2007
21. Majumdar, Alok and Steadman, Todd, "Numerical Modeling of Pressurization of a Propellant Tank", Journal of Propulsion and Power, Vol 17, No.2. March – April, 2001.
22. Steadman, T., Majumdar, A. K. and Holt K., "Numerical Modeling of Helium Pressurization System of Propulsion Test Article (PTA)", 10th Thermal Fluid Analysis Workshop, September 13 – 17, 1999, Huntsville, Alabama.
23. Majumdar, Alok, Valenzuela, Juan, LeClair, Andre and Moder, Jeff, "Numerical modeling of self-pressurization and pressure control by a thermodynamic vent system in a cryogenic tank", Cryogenics, Vol 74, 2016, pp 113-122.
24. Lee, N.H. and Martin, C.S., "Experimental and Analytical Investigation of Entrapped Air in a Horizontal Pipe", Proc. 3rd ASME/JSME Joint Fluids Engg. Conference, ASME, NY, 1999, pp 1-8.
25. Bandyopadhyay, A., Majumdar, A. "Network Flow Simulation of Fluid Transients in Rocket Propulsion Systems," *J. Prop. Power*, Vol. 30, No. 6, pp. 1646–1653, 2014.
26. Bandyopadhyay, A., Majumdar, A, Holt, K. "Fluid Transient Analysis During Priming of Evacuated Line", AIAA 2017-5004, 53rd AIAA/SAE/ASEE Joint Propulsion Conference, 10-12 July 2017, Atlanta, GA
27. Cross, Matthew, Majumdar, Alok, Bennett, John & Malla, Ramesh, "Modeling of Chill Down in Cryogenic Transfer Lines", Journal of Spacecraft and Rockets, Vol. 39, No. 2, pp 284-289, 2002
28. Majumdar, Alok and Ravindran, S.S., "Numerical Modeling of Conjugate Heat Transfer in Fluid Network", *Journal of Propulsion and Power,* Volume 27(3), pp.620-630, 2011.
29. Miropolskii, Z. L.,"Heat Transfer in Film Boiling of a Steam-Water Mixture in Steam Generating Tubes", Teploenergetica, Vol.10,No.5,1963,pp.49-52(in Russian;translation Atomic Energy Commission,AEC-TR-6252, 1964).
30. Brennan, J. A., Brentari, E. G., Smith, R. V., and Steward, W. G., "Cooldown of Cryogenic Transfer Lines—An Experimental Report," National Bureau of Standards Report 9264, November 1966.
31. Darr, S. R., Hu, H., Glikin, N.G., Hartwig, J.W., Majumdar, A.K., LeClair, A.C., and Chung, J.N., "An experimental study on terrestrial cryogenic transfer line chilldown I. Effect of mass flux, equilibrium quality, and inlet subcooling," International Journal of Heat and Mass Transfer, Vol. 103, pp 1225–1242, 2016.
32. LeClair, Andre, C., Hartwig, Jason, W., Hauser, Daniel M., Kassemi Mohammad, Diaz-Hyland, Pablo G,, Going, Thomas R., "Modeling Cryogenic Chilldown of a Transfer Line with the Generalized Fluid System Simulation Program", AIAA Paper no.10.2514/6.2018-4756, AIAA Joint Propulsion Conference, July 9-11, 2018, Cincinnati, Ohio.

Symbol	Description
A	Area (in^2)
C_L	Flow Coefficient
$c_{i,k}$	Mass Concentration of k^{th} Specie at i^{th} Node
c_p	Specific Heat (Btu/lb ^oF)
D	Diameter (in)
f	Darcy Friction Factor
g	Gravitational Acceleration (ft/ sec^2)
g_c	Conversion Constant (= 32.174 lb-ft/lb_f-sec^2)
h	Enthalpy (Btu/lb)
h_{ij}	Heat Transfer Coefficient (Btu/ft^2-sec-°R)
J	Mechanical Equivalent of Heat (778 ft-lb_f/Btu)
K_f	Flow Resistance Coefficient (lb_f-sec^2/(lb-ft)^2)
K	Non-dimensional Head Loss Factor
k	Thermal Conductivity (Btu/ft-sec-° R)
L	Length (in)
m	Resident Mass (lb)
$\dot{m}$	Mass Flow Rate (lb/sec)
p	Pressure (lb_f/ in^2)
Pr	Prandtl Number
Q, q	Heat Source (Btu/sec)
Re	Reynolds Number (Re = ρuD/μ)
R	Gas Constant (lb_f-ft/lb-R)
r	Radius (in)
S	Momentum Source (lb_f)
s	Entropy (Btu/lb-R)
T	Fluid Temperature (^{o} F)
T_s	Solid Temperature (^{o} F)
u	Velocity (ft/sec)
V	Volume (in^3)
x	Quality and Mass Fraction
z	Compressibility Factor

Greek

ρ	Density (lb/ft^3)
θ	Angle Between Branch Flow Velocity Vector and Gravity Vector (deg),
ω	Angular Velocity (rad/sec)
ε	Absolute Roughness (in)
ε_{ij}	Emissivity
ε/D	Relative Roughness
Δh	Head Loss (ft)
μ	Viscosity (lb/ft-sec)
ν	Kinematic Viscosity (ft^2/sec)